Cross-talk dynamics of optical solitons in a broadband Kerr nonlinear system with weak cubic loss

Avner Peleg and Quan M. Nguyen
Department of Mathematics, State University of New York at Buffalo, Buffalo, New York 14260, USA

Yeojin Chung
Department of Mathematics, Southern Methodist University, Dallas, Texas 75275, USA

(Received 20 October 2010; published 29 November 2010)

We study the dynamics of fast soliton collisions in a Kerr nonlinear optical waveguide with weak cubic loss. We obtain analytic expressions for the amplitude and frequency shifts in a single two-soliton collision and show that the impact of a fast three-soliton collision is given by the sum of the two-soliton interactions. Our analytic predictions are confirmed by numerical simulations with the perturbed nonlinear Schrödinger (NLS) equation. Furthermore, we show that the deterministic collision-induced dynamics of soliton amplitudes in a broadband waveguide system with N frequency channels is described by a Lotka-Volterra model for N competing species. For a two-channel system we find that stable transmission with equal prescribed amplitudes can be achieved by a proper choice of linear amplifier gain. The predictions of the Lotka-Volterra model are confirmed by numerical solution of a perturbed coupled-NLS model.

DOI: 10.1103/PhysRevA.82.053830 PACS number(s): 42.65.Tg, 42.81.Dp, 42.65.Sf

I. INTRODUCTION

Broadband optical waveguide communication systems have been the subject of intensive research in recent years due to the ever-increasing demand for high transmission capacity [1–3]. Transmission of information in such systems is often based on the wavelength-division-multiplexing (WDM) method, where many pulse sequences propagate through the same optical waveguide. Each pulse sequence is characterized by the central frequency of its pulses and is hence called a frequency channel. Since pulses from different frequency channels propagate along the waveguide with different group velocities, interchannel pulse collisions are very frequent and can impose severe limitations on transmission quality. On the other hand, it might be possible to find ways to beneficially employ the significant cumulative collision-induced effects in broadband waveguide systems for control and tuning of optical pulse properties such as energy, frequency, and phase.

In this work we focus attention on waveguide-based systems in which the main physical processes are due to second-order dispersion, Kerr nonlinearity, and weak cubic loss. We assume that linear loss either is negligible or is compensated by distributed Raman amplification. The waveguide's cubic loss can be a result of two-photon absorption (TPA) or gain and loss saturation. Pulse propagation in optical waveguides in the presence of two-photon absorption or cubic loss has been studied in many previous works [4–14]. The subject received renewed attention in recent years due to the importance of TPA in silicon nanowaveguides, which are expected to play a crucial role in optical processing applications in optoelectronic devices, including pulse switching and compression, wavelength conversion, regeneration, etc. [15–22]. It is known that the most important effect of a fast interchannel collision in the presence of cubic loss is a decrease in the energy of the colliding pulses [17,20]. This effect, which is known as TPA-induced cross talk, has been demonstrated in recent experiments in silicon nanowaveguide WDM systems [23]. In the experiments reported in Ref. [23] it was shown that TPA-induced cross talk can lead to relatively high values of the bit error rate for sufficiently high power levels of the optical pulses even in a two-channel system.

Despite the great interest in TPA and cubic-loss cross talk in broadband waveguide transmission, a comprehensive analytic study of the phenomenon is still lacking. In the current paper we address important aspects of this problem. We consider conventional solitons of the nonlinear Schrödinger (NLS) equation as an example for the optical pulses and employ an adiabatic perturbation procedure that is suitable for dealing with *fast* soliton collisions in the presence of *weak* perturbations [24–28]. Our perturbative calculations show that the TPA-induced amplitude shift in a *single fast* two-soliton collision is proportional to $\epsilon/|\beta|$, where ϵ is the cubic-loss coefficient and β is the difference between the central frequencies of the colliding pulses. Furthermore, we find that the cross talk is accompanied by a collision-induced frequency shift that scales as $\epsilon/(|\beta|\beta)$. Additionally, for typical broadband transmission systems, in which $|\beta| \gg 1$, the amplitude shift in a fast three-soliton collision is given by a sum over the two-soliton interactions. Our analytic results for the single two-soliton and three-soliton collision are confirmed by numerical solution of the perturbed NLS equation with the cubic-loss term.

Since in broadband WDM transmission systems the frequency difference between the lowest and highest frequency channels is large, the corresponding group velocity difference is also large. Thus, each optical pulse might undergo a large number of interchannel collisions during the transmission. It is therefore important to obtain an accurate description of pulse dynamics under many interchannel collisions. In the current study we tackle this problem by developing a reduced model for the deterministic evolution of pulse amplitudes in soliton-based broadband transmission with N frequency channels. The derivation of the reduced model is based on the analysis of a single interchannel collision and on the assumptions that the solitons in each frequency channel are well separated in time and that radiation emission effects can be neglected. Under these assumptions we show that

the cross-talk-induced amplitude dynamics in an N-channel transmission line is described by a Lotka-Volterra model for N competing species. Furthermore, for a two-channel system we show that stable stationary transmission with equal prescribed amplitudes can be achieved by a proper choice of linear amplifier gain. In addition, we find the conditions on the time slot width and the soliton's equilibrium amplitude value under which the transmission is indeed stable. The predictions of the reduced Lotka-Volterra model are confirmed by numerical solution of a coupled-NLS model, which takes into account intrapulse and interpulse effects due to Kerr nonlinearity and cubic loss.

Our reasons for considering optical solitons as an example for the propagating pulses are the following. First, in many of the systems under consideration the waveguides are highly nonlinear, and pulse propagation is accurately described by a perturbed NLS equation [6,7,9,17,18,20]. Furthermore, NLS-type solitons were experimentally demonstrated in quite a few of these systems [12,19,21,29,30]. Second, since the unperturbed NLS equation is an integrable model [31] and since optical solitons are stable stationary solutions of this model, derivation of analytic results for the effects of cubic loss on interpulse collisions can be done in a rigorous manner. Third, due to their properties, optical solitons are considered to be ideal candidates for information transmission and processing in broadband waveguide systems [1].

The rest of the paper is organized as follows. In Sec. II we briefly review the perturbation procedure developed in Refs. [24,25] and employ it to calculate the main effects of cubic loss on a single fast two- and three-soliton collision. In Sec. III we present the results of numerical simulations of a single two- and three-soliton collision as well as of two successive two-soliton collisions. We also analyze these results in comparison with the analytic predictions obtained in Sec. II. The reduced model for the dynamics of soliton amplitudes in an N-channel transmission line is developed in Sec. IV A. In Sec. IV B we provide a detailed analysis of amplitude dynamics in a two-channel system and obtain the conditions for stable transmission. In addition, we compare the predictions of the reduced model with results of numerical simulations with a perturbed coupled-NLS model. Section V gives our conclusions.

II. EFFECTS OF CUBIC LOSS ON A SINGLE TWO- AND THREE-SOLITON COLLISION

A. Basic equations

Propagation of pulses of light through an optical waveguide in the presence of second-order dispersion, Kerr nonlinearity, and weak cubic loss can be described by the following perturbed NLS equation [6,7,17]:

$$i\partial_z\psi + \partial_t^2\psi + 2|\psi|^2\psi = -i\epsilon|\psi|^2\psi, \tag{1}$$

where ψ is proportional to the envelope of the electric field, z is propagation distance, and t is time in the retarded reference frame. The term $-\epsilon|\psi|^2\psi$ describes the effects of cubic loss, and ϵ is the cubic-loss coefficient. The cubic-loss term on the right-hand side of Eq. (1) is often associated with two-photon absorption. We assume here that linear loss is compensated by distributed Raman amplification [32–37]. The fundamental soliton solution of the unperturbed NLS equation with central frequency β is

$$\psi_\beta(t,z) = \eta_\beta \frac{\exp(i\chi_\beta)}{\cosh(x_\beta)}, \tag{2}$$

where $x_\beta = \eta_\beta(t - y_\beta - 2\beta z)$, $\chi_\beta = \alpha_\beta + \beta(t - y_\beta) + (\eta_\beta^2 - \beta^2)z$, and η_β,α_β, and y_β are the soliton amplitude, phase, and position, respectively.

Let us describe the effects of cubic loss on single-soliton propagation. Employing the standard adiabatic perturbation theory for the NLS soliton [38] we obtain the following equation for the dynamics of its amplitude:

$$\frac{d\eta^{(s)}(z)}{dz} = -\frac{4}{3}\epsilon\eta^{(s)3}(z), \tag{3}$$

where the superscript s denotes self-amplitude shift, that is, an amplitude shift which is due to single-pulse propagation. Thus, the z dependence of the soliton's amplitude is given by the following equation [6,7]:

$$\eta^{(s)}(z) = \frac{\eta(0)}{[1 + 8\epsilon\eta^2(0)z/3]^{1/2}}. \tag{4}$$

B. Two-soliton collision

Next, we consider the effects of cubic loss on a single two-soliton collision. For simplicity and without loss of generality, the central frequencies of the solitons are taken as $\beta = 0$ and β. We refer to these solitons as the reference-channel soliton and the β-channel soliton, respectively. Since we are interested in a fast collision in the presence of weak cubic loss we assume that $\epsilon \ll 1$ and $1/|\beta| \ll 1$. In addition, we assume that the two solitons are initially well separated from each other in the temporal domain. Under these assumptions we can employ the perturbation technique, developed in Refs. [24,25], and successfully applied for studying soliton collisions in the presence of third-order dispersion [24,25], quintic nonlinearity [26], and delayed Raman response [27,28,39–41]. Following this perturbation technique, we look for a two-pulse solution of Eq. (1) in the form

$$\psi_{\text{two}} = \psi_0 + \psi_\beta + \phi, \tag{5}$$

where ψ_0 and ψ_β are single-soliton solutions of Eq. (1) with $0 < \epsilon \ll 1$ in channels 0 and β, respectively. The term ϕ on the right-hand side of Eq. (5) represents a small correction to the single-soliton solutions, which is solely due to collision effects. In analogy with the ideal collision case we express ϕ as

$$\phi = \phi_0 + \phi_\beta + \cdots, \tag{6}$$

where ϕ_0 and ϕ_β describe collision-induced effects in channels 0 and β, and the ellipsis represents higher-order terms in other channels. Combining Eqs. (5) and (6) we observe that the envelope of the reference-channel pulse is $\psi_0^{\text{total}} = \psi_0 + \phi_0$.

We now substitute the relations (5) and (6) together with $\psi_0(t,z) = \Psi_0(x_0)\exp(i\chi_0)$, $\phi_0(t,z) = \Phi_0(x_0)\exp(i\chi_0)$, $\psi_\beta(t,z) = \Psi_\beta(x_\beta)\exp(i\chi_\beta)$, and $\phi_\beta(t,z) = \Phi_\beta(x_\beta)\exp(i\chi_\beta)$ into Eq. (1) and keep terms up to $O(\epsilon/\beta)$. As we show in the following, this approximation allows us to calculate

collision-induced effects up to $O(\epsilon/\beta^2)$. Since ϕ_0 and ψ_0 oscillate with the same frequency, and since $|\beta| \gg 1$, the resulting equation readily decomposes into an equation for the evolution of Φ_0 and an equation for the evolution of Φ_β [24,26,27]. We focus attention on Φ_0 and comment that the calculation of Φ_β is similar. The equation for Φ_0 is

$$\begin{aligned} i\partial_z\Phi_0 + \left[\left(\partial_t^2 - \eta_0^2\right)\Phi_0 + 4|\Psi_0|^2\Phi_0 + 2\Psi_0^2\Phi_0^*\right] \\ = -4[|\Psi_\beta|^2\Psi_0 + |\Psi_\beta|^2\Phi_0 + \Psi_0(\Psi_\beta\Phi_\beta^* + \Psi_\beta^*\Phi_\beta)] \\ - 2i\epsilon\left[|\Psi_\beta|^2\Psi_0 + |\Psi_0|^2\Phi_0 + \Psi_0^2\Phi_0^*/2 + |\Psi_\beta|^2\Phi_0\right. \\ \left. + \Psi_0(\Psi_\beta\Phi_\beta^* + \Psi_\beta^*\Phi_\beta)\right]. \end{aligned} \tag{7}$$

The field Φ_0 is obtained in the form of a perturbation series. That is, we substitute

$$\begin{aligned} \Phi_0(x_0,z) = \Phi_{01}^{(0)}(x_0,z) + \Phi_{01}^{(1)}(x_0,z) + \Phi_{02}^{(0)}(x_0,z) \\ + \Phi_{02}^{(1)}(x_0,z) + \cdots \end{aligned} \tag{8}$$

into Eq. (7) and expand the result with respect to ϵ and $1/\beta$. In Eq. (8) the first subscript in $\Phi_{01}^{(0)}$, for example, stands for the channel, the second subscript indicates the combined order with respect to both ϵ and $1/\beta$, and the superscript represents the order in ϵ. The total collision-induced change in the reference-channel soliton's envelope is $\Delta\Phi_0(x_0) = \Phi_0(x_0,\infty) - \Phi_0(x_0,-\infty)$. The corresponding changes in soliton parameters are calculated by projecting $\Delta\Phi_0(x_0)$ onto one of the four localized eigenmodes of the linear operator $\hat{L}$ describing small perturbations about the fundamental NLS soliton [24,26,27].

Turning to the results of the perturbative calculations, we note that the only collision-induced effects in orders $1/\beta$ and $1/\beta^2$ are a phase shift $\Delta\alpha_0 = 4\eta_\beta/|\beta|$ and a position shift $\Delta y_0 = -4\eta_\beta/(\beta|\beta|)$. Both effects already exist in the unperturbed two-soliton collision [31]. In addition, there are no terms of order $\epsilon\beta$ on the right-hand side of Eq. (7), and as a result, there are no effects in order ϵ. We therefore start the discussion of perturbative calculations by considering the effects of the collision in order ϵ/β. In this order Eq. (7) is reduced to

$$i\partial_z\Phi_{02}^{(1)} = -2i\epsilon|\Psi_\beta|^2\Psi_0. \tag{9}$$

Integration over z yields

$$\Delta\Phi_{02}^{(1)}(x_0) = -\frac{2\epsilon\eta_0\eta_\beta}{|\beta|\cosh(x_0)}. \tag{10}$$

To obtain the collision-induced amplitude shift we project $(\Delta\Phi_{02}^{(1)}(x_0), \Delta\Phi_{02}^{(1)*}(x_0))^T$ on the eigenfunction $f_0(x_0) = \mathrm{sech}(x_0)(1,-1)^T$ of the operator $\hat{L}$ and integrate over x_0 (see Ref. [27] for a similar calculation). This calculation yields the following expression for the amplitude shift $\Delta\eta_0^{(c)}$ induced by cubic-loss cross talk:

$$\Delta\eta_0^{(c)} = -4\epsilon\eta_0\eta_\beta/|\beta|. \tag{11}$$

As we show in the following, the fact that $\Delta\eta_0^{(c)}$ is inversely proportional to $|\beta|$ means that in N-channel transmission systems the cumulative amplitude shift induced by the cross talk is proportional to $N\epsilon$. Therefore, in WDM systems with a large number of channels, cubic-loss cross-talk effects are dominant compared with the effects of cubic loss on single-pulse propagation as described by Eq. (4).

We now turn to describe collision-induced effects in order ϵ/β^2. This calculation is of particular interest since it reveals that the presence of cubic loss leads to a shift of the central frequencies of the colliding solitons. We refer to this frequency shift as the cubic-loss cross-frequency shift. Taking into account all terms of order ϵ/β in Eq. (7) we arrive at the equation

$$\begin{aligned} i\partial_z\Phi_{03}^{(1)} = -\left[\left(\partial_t^2 - \eta_0^2\right)\Phi_{02}^{(1)} + 4|\Psi_0|^2\Phi_{02}^{(1)} + 2\Psi_0^2\Phi_{02}^{(1)*}\right] \\ - 4|\Psi_\beta|^2\Phi_{02}^{(1)} - 4\Psi_0\left(\Psi_\beta\Phi_{\beta 2}^{(1)*} + \Psi_\beta\Phi_{\beta 2}^{(1)}\right) \\ - 2i\epsilon\left[|\Psi_0|^2\Phi_{01}^{(0)} + \Psi_0^2\Phi_{01}^{(0)*}/2 + |\Psi_\beta|^2\Phi_{01}^{(0)}\right. \\ \left. + \Psi_0\left(\Psi_\beta\Phi_{\beta 1}^{(0)*} + \Psi_\beta\Phi_{\beta 1}^{(0)}\right)\right]. \end{aligned} \tag{12}$$

It is possible to show that the only terms on the right-hand side of Eq. (12) that contribute to the integral over z are the dispersion term $-\partial_t^2\Phi_{02}^{(1)}$ and the cross-phase modulation term $-4\Psi_0(\Psi_\beta\Phi_{\beta 2}^{(1)*} + \Psi_\beta\Phi_{\beta 2}^{(1)})$. Substituting the expressions for Ψ_0, Ψ_β, $\Phi_{01}^{(0)}$, $\Phi_{\beta 1}^{(0)}$, $\Phi_{02}^{(1)}$, and $\Phi_{\beta 2}^{(1)}$, we obtain the following equation for $\Phi_{03}^{(1)}$:

$$i\partial_z\Phi_{03}^{(1)} = \frac{10\epsilon\eta_0^2\eta_\beta^2}{\beta}\frac{\tanh(x_0)}{\cosh(x_0)\cosh^2(x_\beta)}. \tag{13}$$

We note that the contributions of the dispersion and cross-phase modulation terms have the same sign. This is different from the case of the Raman-induced cross-frequency shift, where dispersion and Kerr nonlinearity give contributions of opposite signs [27]. Integration over propagation distance yields

$$\Delta\Phi_{03}^{(1)}(x_0) = \frac{-10i\epsilon\eta_0^2\eta_\beta}{|\beta|\beta}\frac{\tanh(x_0)}{\cosh(x_0)}. \tag{14}$$

The collision-induced frequency shift is calculated by projecting $(\Delta\Phi_{03}^{(1)}(x_0), \Delta\Phi_{03}^{(1)*}(x_0))^T$ on the eigenfunction $f_1(x_0) = \sinh(x_0)\mathrm{sech}^2(x_0)(1,1)^T$ of the operator $\hat{L}$ and integrating over x_0:

$$\Delta\beta_0^{(c)} = -\frac{20\epsilon\eta_0^2\eta_\beta}{3|\beta|\beta}. \tag{15}$$

C. Three-soliton collision

In multichannel waveguide transmission systems, where the pulses are ordered in periodic sequences, effects of collisions between three or more pulses all from different channels might become important. Since Eq. (1) contains terms that are either linear or cubic in ψ, one can expect that consideration of three-soliton collisions would be sufficient for an accurate description of the dynamics induced by many-soliton collisions. We therefore turn to study this case.

As an example, we consider a fast collision involving solitons with central frequencies β, 0, and $-\beta$. We assume that $\epsilon \ll 1$, $1/|\beta| \ll 1$, and $y_\beta(0) = -y_{-\beta}(0)$ and that the three solitons are initially well separated in time. We look for a three-pulse solution of Eq. (1) in the form

$$\psi_{\mathrm{three}} = \psi_0 + \psi_\beta + \psi_{-\beta} + \phi_0 + \phi_\beta + \phi_{-\beta} + \cdots, \tag{16}$$

where $\psi_{-\beta}$ is the single pulse solution in the $-\beta$ channel, $\phi_{-\beta}$ describes collision-induced effects in the $-\beta$ channel, and the ellipsis represents higher-order terms in other channels. We substitute relation (16) along with $\psi_0(t,z) = \Psi_0(x_0)\exp(i\chi_0)$, $\phi_0(t,z) = \Phi_0(x_0)\exp(i\chi_0)$, $\psi_\beta(t,z) = \Psi_\beta(x_\beta)\exp(i\chi_\beta)$, $\phi_\beta(t,z) = \Phi_\beta(x_\beta)\exp(i\chi_\beta)$, $\psi_{-\beta}(t,z) = \Psi_{-\beta}(x_{-\beta})\exp(i\chi_{-\beta})$, and $\phi_{-\beta}(t,z) = \Phi_{-\beta}(x_{-\beta})\exp(i\chi_{-\beta})$ into Eq. (1) and keep terms up to first order with respect to both ϵ and $1/\beta$. This allows us to calculate collision effects up to second order. Exploiting the fact that $|\beta| \gg 1$ we obtain the following equation for Φ_0:

$$\begin{aligned} &i\partial_z\Phi_0 + \left[\left(\partial_t^2 - \eta_0^2\right)\Phi_0 + 4|\Psi_0|^2\Phi_0 + 2\Psi_0^2\Phi_0^*\right] \\ &\quad = -4(|\Psi_\beta|^2 + |\Psi_{-\beta}|^2)(\Psi_0 + \Phi_0) \\ &\qquad - 4\Psi_0[(\Psi_\beta\Phi_\beta^* + \Psi_\beta^*\Phi_\beta) + (\Psi_{-\beta}\Phi_{-\beta}^* + \Psi_{-\beta}^*\Phi_{-\beta})] \\ &\qquad - 4[\Psi_0^*(\Psi_\beta\Psi_{-\beta} + \Psi_\beta\Phi_{-\beta} + \Phi_\beta\Psi_{-\beta}) + \Phi_0^*\Psi_\beta\Psi_{-\beta}] \\ &\qquad \times \exp(-2i\chi_0 + i\chi_\beta + i\chi_{-\beta}) - 2i\epsilon(|\Psi_\beta|^2 + |\Psi_{-\beta}|^2)\Psi_0 \\ &\qquad - 2i\epsilon\Psi_0^*\Psi_\beta\Psi_{-\beta}\exp(-2i\chi_0 + i\chi_\beta + i\chi_{-\beta}). \end{aligned} \tag{17}$$

We substitute the expansion in Eq. (8) into Eq. (17) and keep terms up to second order. We observe that the only collision-induced effects in orders $1/\beta$ and $1/\beta^2$ are a phase shift $\Delta\alpha_0$ and a position shift Δy_0. When $|\beta| \gg 1$ and the soliton amplitudes are of order 1 these phase and position shifts are given by $\Delta\alpha_0 = 4(\eta_\beta + \eta_{-\beta})/|\beta|$ and $\Delta y_0 = -4(\eta_\beta - \eta_{-\beta})/(\beta|\beta|)$, respectively. Thus, the phase shift and position shift in the three-soliton collision are given by a sum over two-soliton interaction effects, in accordance with Ref. [31]. In addition, there are no collision-induced effects in order ϵ. The equation describing the dynamics in order ϵ/β is

$$\begin{aligned} i\partial_z\Phi_{02}^{(1)} &= -2i\epsilon(|\Psi_\beta|^2 + |\Psi_{-\beta}|^2)\Psi_0 \\ &\quad - 2i\epsilon\Psi_0^*\Psi_\beta\Psi_{-\beta}\exp(-2i\chi_0 + i\chi_\beta + i\chi_{-\beta}). \end{aligned} \tag{18}$$

The first two terms on the right-hand side of Eq. (18) are clearly associated with two-soliton interaction. Therefore, the only contribution to $\Delta\Phi_{02}^{(1)}$ from three-soliton interaction can come from the third term. Denoting this contribution by $\Delta\Phi_{02}^{(1)3b}$ and integrating over z, we obtain

$$\Delta\Phi_{02}^{(1)3b}(x_0) = -2\epsilon\Psi_0 I_{02}^{(1)3b}(t)\exp[i\chi^{3b}(0)], \tag{19}$$

where

$$\begin{aligned} I_{02}^{(1)3b}(t) &= \int_{-\infty}^{\infty} dz\Psi_\beta(t,z)\Psi_{-\beta}(t,z) \\ &\quad \times \exp\left[i\left(2\beta^2 + \eta_\beta^2 + \eta_{-\beta}^2 - 2\eta_0^2\right)z\right], \end{aligned} \tag{20}$$

and $\chi^{3b}(0) = \alpha_\beta(0) + \alpha_{-\beta}(0) - 2\alpha_0(0) - \beta[y_\beta(0) - y_{-\beta}(0)]$. For a typical broadband transmission system, $|\beta| \gg 1$, while η_0, η_β, and $\eta_{-\beta}$ are of order 1. In this case, the oscillation period of the exponential function appearing in the integral on the right-hand side of Eq. (20) can be estimated by $z_{\rm osc} = \pi/|\beta|^2$. The collision length can be estimated by $z_{\rm col} = 1/|\beta|$. Thus, the oscillations of the integrand in Eq. (20) will make $\Delta\Phi_{02}^{(1)3b}$ small if $z_{\rm osc} \ll z_{\rm col}$, or equivalently, if $|\beta| \gg \pi$. In order to verify this argument we calculate $I_{02}^{(1)3b}(t)$ numerically with $\eta_0 = \eta_\beta = \eta_{-\beta} = 1$ for $\beta = 10$, $\beta = 5$, and $\beta = 1$. The results are shown in Fig. 1.

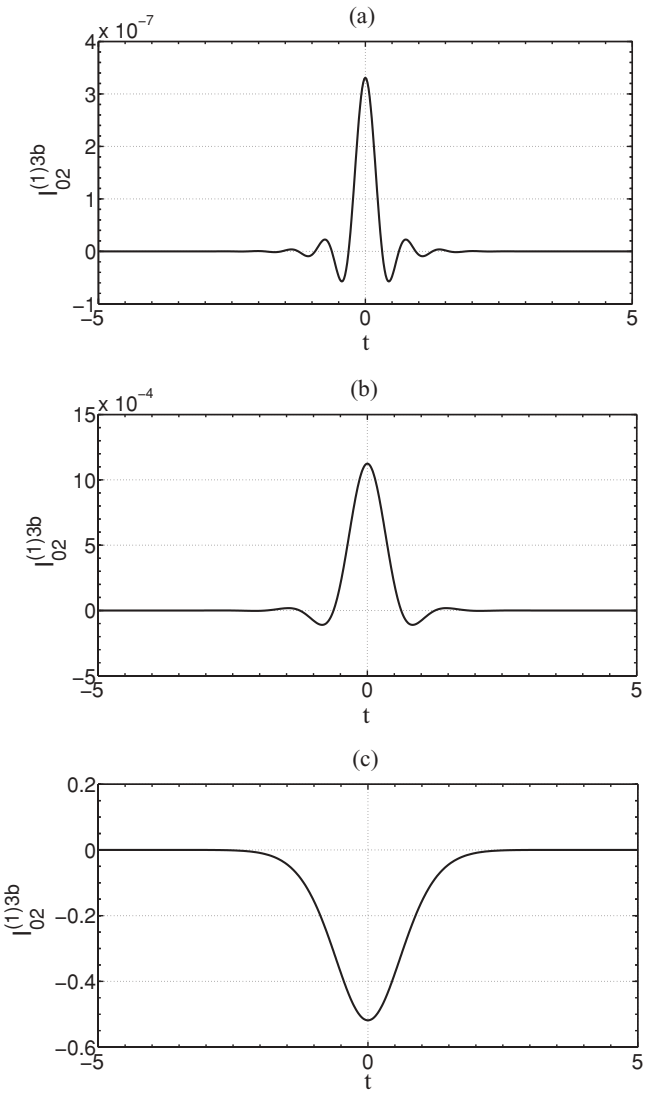

FIG. 1. The integral $I_{02}^{(1)3b}$ vs time t for $\eta_0 = \eta_\beta = \eta_{-\beta} = 1$ and $\beta = 10$ (a), $\beta = 5$ (b), and $\beta = 1$ (c).

Based on this discussion we conclude that when $|\beta| \gg 1$ and η_0, η_β, and $\eta_{-\beta}$ are of order 1, the amplitude shift $\Delta\eta_0^{(c)}$ in a three-soliton collision is given by a sum of the amplitude shifts due to two-soliton interaction:

$$\Delta\eta_0^{(c)} = -4\epsilon\eta_0(\eta_\beta + \eta_{-\beta})/|\beta|. \tag{21}$$

A similar calculation shows that the same conclusion is valid for the collision-induced amplitude shifts $\Delta\eta_\beta^{(c)}$ and $\Delta\eta_{-\beta}^{(c)}$.

III. NUMERICAL SIMULATIONS

The analytic predictions for the soliton amplitude and cross-frequency shifts in Eqs. (11), (15), and (21) are based on the assumption that radiation emission effects can be neglected. We remark that emission of continuous waves due to single-soliton propagation affects the soliton parameters in order ϵ^2 (see Refs. [42,43], for example). Therefore, Eq. (11) for the collision-induced amplitude shift is expected to hold when $\epsilon^2 \ll \epsilon/|\beta| \ll 1$ or, equivalently, when $\epsilon \ll 1/|\beta| \ll 1$.

In addition, Eq. (15) for the soliton cross-frequency shift is expected to hold when $\epsilon^2 \ll \epsilon/|\beta|^2 \ll 1$ or, equivalently, when $\epsilon \ll 1/|\beta|^2 \ll 1$.

In order to validate the analytic predictions in the previous section we perform numerical simulations with Eq. (1). The equation is integrated by employing a split-step method that is of fourth order with respect to the step size in z [44]. The step sizes in t and z are taken as $\Delta t = 0.005$ and $\Delta z = 0.004$, respectively. The size of the computational domain is $-1000 \leqslant t \leqslant 1000$, and the number of Fourier modes is 1.28×10^6 so that the spacing between adjacent points of the frequency grid is $\Delta\omega = 0.001$. The small frequency spacing and large number of Fourier modes allow us to accurately measure frequency shifts of order 10^{-3}, which is the value of the cross-frequency shift that is expected from Eq. (15) for $\epsilon = 0.04$ and $|\beta| > 10$.

In simulating a single two-soliton collision we take the initial condition as the sum of two fundamental solitons of the form (2) with frequencies $\beta = 0$ and β. The values of $|\beta|$ are in the range $1 \leqslant |\beta| \leqslant 25$. The initial positions of the solitons are $y_0(0) = 0$, $y_\beta(0) = -15$ for $\beta > 0$, and $y_\beta(0) = 15$ for $\beta < 0$; i.e., the two solitons are initially well separated in the time domain. The initial amplitudes and phases of the two solitons are $\eta_0(0) = \eta_\beta(0) = 1$ and $\alpha_0(0) = \alpha_\beta(0) = 0$, respectively. The simulations are carried out up to a final distance z_f, such that $1 \leqslant z_f \leqslant 8$ and $|y_\beta(z_f) - y_0(z_f)| \gg 1$. Thus, the two solitons are well separated in the time domain at z_f.

The β dependence of the collision-induced amplitude shift $\Delta\eta_0^{(c)}$ obtained by numerical simulations with $\epsilon = 0.02$ and $\epsilon = 0.05$ is shown in Fig. 2 along with the analytic prediction of Eq. (11). The numerical results are in very good agreement with the analytic prediction for frequency difference values $|\beta| \geqslant 5$. For smaller values of $|\beta|$, for which the assumptions of the perturbation theory are not satisfied, the numerically obtained values of $|\Delta\eta_0^{(c)}|$ can deviate from the values predicted by Eq. (11). When $1 < \beta < 5$ the numerical results for $|\Delta\eta_0^{(c)}|$ are significantly smaller compared with the analytic prediction for both $\epsilon = 0.02$ and $\epsilon = 0.05$, while for $-5 < \beta < -1$ and $\epsilon = 0.05$ the numerical results for $|\Delta\eta_0^{(c)}|$ are larger than the analytic prediction. Surprisingly, when $\epsilon = 0.02$ we observe good agreement between simulations and theory even for $-5 < \beta < -1$.

Figure 3 shows the β dependence of the collision-induced frequency shift experienced by the reference-channel soliton $\Delta\beta_0^{(c)}$ for $\epsilon = 0.04$. We observe good agreement between the result obtained by numerical simulations with Eq. (1) and the analytic prediction of Eq. (15). Thus, we conclude that a fast two-soliton collision in the presence of cubic loss induces an $O(\epsilon/\beta^2)$ frequency shift.

As explained in Sec. I, in broadband communication systems many pulse sequences, each characterized by the central frequency of its pulses, propagate through the same waveguide. In this case a pulse in a given sequence typically undergoes many consecutive collisions with pulses from other sequences. It is therefore interesting to investigate whether or not the impact of successive two-pulse collisions can be described by summing over the individual collisions. As an example, we consider the effects of two consecutive collisions of a reference-channel soliton with two β-channel solitons.

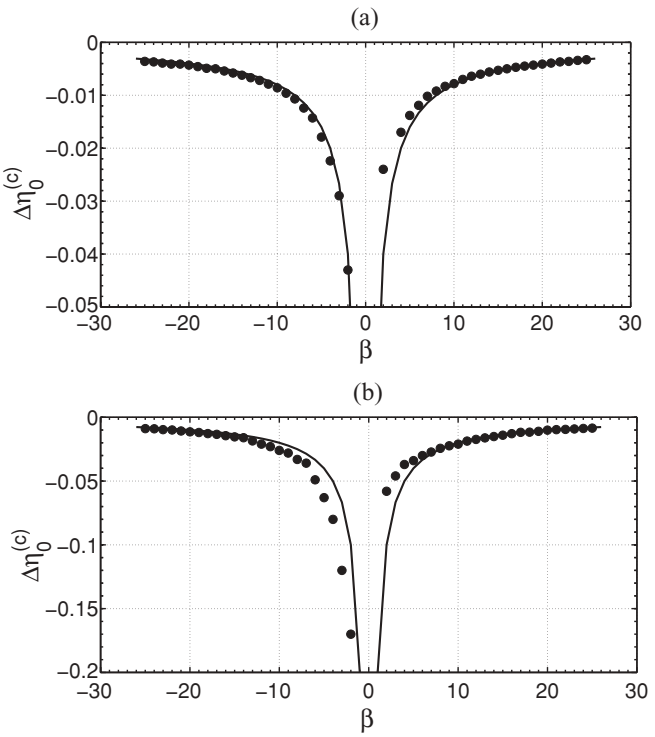

FIG. 2. Collision-induced amplitude shift of the reference-channel soliton $\Delta\eta_0^{(c)}$ as a function of the frequency difference β for $\epsilon = 0.02$ (a) and $\epsilon = 0.05$ (b). The circles represent the result of numerical simulations with Eq. (1), and the solid line stands for the analytic prediction of Eq. (11).

The initial parameters of the reference-channel soliton are $\eta_0(0) = 1$, $y_0(0) = 0$, and $\alpha_0(0) = 0$, while those of the two β-channel solitons are $\eta_{\beta 1}(0) = \eta_{\beta 2}(0) = 1$, $y_{\beta 1}(0) = -10$, $y_{\beta 2}(0) = -20$, and $\alpha_{\beta 1}(0) = \alpha_{\beta 2}(0) = 0$. Thus, the three solitons are initially well separated in the time domain. In addition, the total amplitude shift of the reference-channel soliton induced by the two collisions is calculated at a distance z_f at which the solitons are again well separated. The actual values of z_f are $1 \leqslant z_f \leqslant 12$, depending on the value of β. The numerically obtained dependence of the

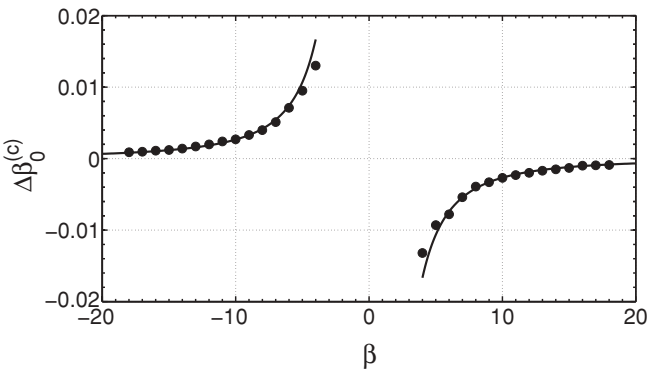

FIG. 3. Collision-induced frequency shift of the reference-channel soliton $\Delta\beta_0^{(c)}$ as a function of the frequency difference β for $\epsilon = 0.04$. The circles represent the result of numerical simulations with Eq. (1), and the solid line corresponds to the analytic prediction of Eq. (15).

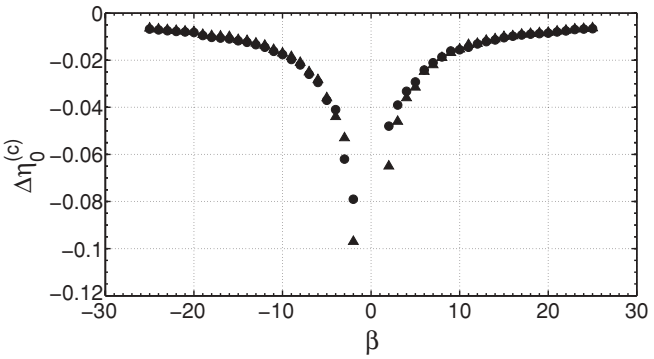

FIG. 4. The total amplitude shift of the reference-channel soliton $\Delta\eta_0^{(c)}$ in two successive collisions with two well-separated β-channel solitons vs frequency difference β for $\epsilon = 0.02$. The circles represent the result of numerical simulations with Eq. (1), and the triangles stand for the analytic prediction of Eq. (22).

total amplitude shift $\Delta\eta_0^{(c)}$ on the frequency difference β for $\epsilon = 0.02$ is shown in Fig. 4. Also shown is the analytic result obtained by employing Eq. (11) and summing over the two collisions:

$$\Delta\eta_0^{(c)} = -4\epsilon[\eta_0(z_1)\eta_{\beta 1}(z_1) + \eta_0(z_2)\eta_{\beta 2}(z_2)]/|\beta|, \qquad (22)$$

where z_1 and z_2 are the collision distances for the first and second collisions, respectively. That is, z_1 and z_2 are the distances at which the envelope of the reference-channel soliton completely overlaps with the envelope of the first and second β-channel soliton. The good agreement between numerical simulations and the result obtained by employing Eq. (22) shows that when the two β-channel solitons are well separated the effects of two consecutive collisions are indeed given by a sum of the effects of the individual collisions.

Next we consider the impact of a three-soliton collision involving solitons from the 0, β, and $-\beta$ channels. The initial parameters of the solitons are $\eta_0(0) = \eta_\beta(0) = \eta_{-\beta}(0) = 1$, $y_0(0) = 0$, $y_\beta(0) = -15$, $y_{-\beta}(0) = 15$, and $\alpha_0(0) = \alpha_\beta(0) = \alpha_{-\beta}(0) = 0$. As discussed in Sec. II C, when $|\beta| \gg 1$ and η_0, η_β, and $\eta_{-\beta}$ are of order 1, the amplitude shift of the reference-channel soliton in the three-soliton collision should be well approximated by Eq. (21). That is, the amplitude shift is given by a sum over the two-body interactions. The β dependence of the amplitude shifts of the reference-channel and β-channel solitons $\Delta\eta_0^{(c)}$ and $\Delta\eta_\beta^{(c)}$ obtained in numerical simulations with $\epsilon = 0.02$ is shown in Fig. 5 along with the theoretical prediction obtained by employing Eq. (21). The agreement between theory and simulations is very good for $|\beta| \geqslant 5$. Surprisingly, good agreement is also observed for $-5 < \beta < -1$, where the perturbation description is not expected to be valid. For $1 < \beta < 5$ the numerically obtained values of the amplitude shifts are significantly larger than the analytic prediction of Eq. (21). Based on these observations we conclude that when $|\beta| \gg 1$ and η_0, η_β, and $\eta_{-\beta}$ are of order 1, the three-soliton interaction can be approximated by summing over the two-soliton interactions.

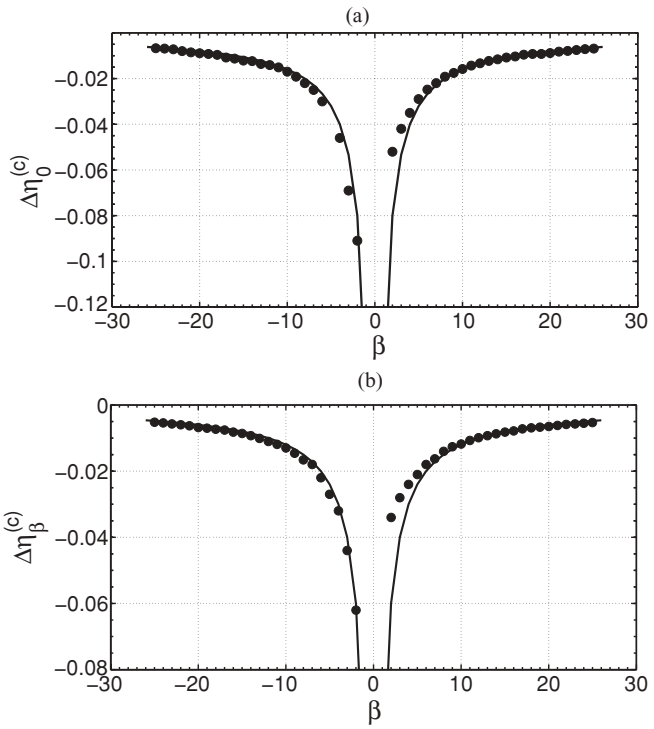

FIG. 5. Amplitude shifts of the 0-channel and β-channel solitons $\Delta\eta_0^{(c)}$ and $\Delta\eta_\beta^{(c)}$ in a three-soliton collision as functions of the frequency difference β for $\epsilon = 0.02$. The circles correspond to the result of numerical simulations with Eq. (1), and the solid line represents the analytic prediction based on Eq. (21). (a) $\Delta\eta_0^{(c)}$ vs frequency difference. (b) $\Delta\eta_\beta^{(c)}$ vs frequency difference.

IV. DETERMINISTIC CROSS-TALK DYNAMICS IN BROADBAND TRANSMISSION SYSTEMS

A. Derivation of the model

We consider a soliton-based multichannel transmission system with N frequency channels and frequency difference $\Delta\beta$ between adjacent channels and develop a reduced model for deterministic amplitude dynamics due to cubic loss. The derivation of the model is similar to the one carried out in Refs. [45,46] for amplitude dynamics induced by Raman cross talk. However, the resulting model and observed dynamics are quite different from those considered in Refs. [45,46]. The model is based on the following assumptions: (1) Information is encoded in the phase so that the soliton sequences in all channels are deterministic; i.e., all time slots are occupied and each soliton is located at the center of a time slot of width T, where $T \gg 1$. The initial amplitudes of all solitons in a given channel are equal, but initial amplitudes of solitons in different channels are not necessarily equal. This setup corresponds, for example, to return-to-zero differential-phase-shift-keyed transmission. (2) The sequences are either (a) infinitely long or (b) subject to periodic temporal boundary conditions. Notice that setup (a) is an approximation for long-haul transmission systems, while setup (b) is an approximation for closed waveguide-loop experiments. (3) We take into account linear and cubic loss, cross talk induced by cubic loss, and distributed linear amplifier gain. Thus, the net linear gain or loss in each channel is determined by the difference between linear

TABLE I. Equilibrium states of Eq. (27) and their properties.

Point	Existence	Stable	Unstable
(η,η)	$\eta > 0$	$\eta > 3/T$	$0 < \eta \leqslant 3/T$
$(0,0)$	$\eta > 0$		$\eta > 0$
$(C^{1/2}(\eta),0)$	$\eta > 0$	$0 < \eta < 3(\sqrt{5}-1)/T$	$\eta \geqslant 3(\sqrt{5}-1)/T$
$(0,C^{1/2}(\eta))$	$\eta > 0$	$0 < \eta < 3(\sqrt{5}-1)/T$	$\eta \geqslant 3(\sqrt{5}-1)/T$
$(C_2(\eta),C_3(\eta))$	$3/T < \eta < 3(\sqrt{5}-1)/T$		$3/T < \eta < 3(\sqrt{5}-1)/T$
$(C_3(\eta),C_2(\eta))$	$3/T < \eta < 3(\sqrt{5}-1)/T$		$3/T < \eta < 3(\sqrt{5}-1)/T$

amplifier gain and linear waveguide loss. (4) Since $T \gg 1$ the pulses in each frequency channel are well separated in time. As a result, intrachannel interaction is exponentially small and is neglected. (5) Radiation emission effects are neglected, in accordance with the analysis of the single collision problem in Secs. II and III.

Since the pulse sequences are periodic, and since the initial amplitudes are equal for all pulses in the same sequence, the parameters of all pulses in a given sequence undergo the same deterministic dynamic evolution. Let us obtain the evolution equation for the amplitude of the jth-channel solitons, for example. For this purpose we note that the distance traveled by these solitons while passing two successive solitons in the $j-1$ or $j+1$ channels is $\Delta z_c^{(1)} = T/(2\Delta\beta)$. We denote by z_l the location of the lth collision of a given jth-channel soliton with solitons in the $j+1$ or $j-1$ channel and note that $z_l = z_{l-1} + \Delta z_c^{(1)}$. Using Eq. (11) and summing over all collisions occurring within the interval $(z_{l-1}, z_{l-1} + \Delta z_c^{(1)}]$, we obtain the equation

$$\eta_j\left(z_{l-1} + \Delta z_c^{(1)}\right) = \eta_j(z_{l-1}) + g_j\eta_j(z_{l-1})\Delta z_c^{(1)} - \frac{4\epsilon}{3}\eta_j^3(z_{l-1})\Delta z_c^{(1)} - \frac{4\epsilon}{\Delta\beta}\sum_{k=1}^{N}(1-\delta_{jk})\eta_j(z_{l-1})\eta_k(z_{l-1}), \tag{23}$$

where g_j is the constant net linear gain or loss for the jth channel and δ_{jk} is the Kronecker delta function. The same equations with different j values, where $j = 1,\ldots,N$, describe the dynamics of the soliton amplitudes in all frequency channels. Going to the continuum limit we obtain

$$\frac{d\eta_j}{dz} = \eta_j\left[g_j - \frac{4\epsilon}{3}\eta_j^2 - \frac{8\epsilon}{T}\sum_{k=1}^{N}(1-\delta_{jk})\eta_k\right]. \tag{24}$$

We recall that in optical fiber communication systems it is often desired to achieve a steady state in which the pulse amplitudes in all channels are equal and constant [1]. We therefore look for a stationary state of the system (24) in the form $\eta_j^{(\mathrm{eq})} = \eta > 0$ for $j = 1,\ldots,N$, where η is the desired equilibrium value of soliton amplitudes. This yields the following expression for g_j:

$$g_j = \frac{4\epsilon}{3}\eta^2 + \frac{8\epsilon}{T}(N-1)\eta. \tag{25}$$

Therefore, the gain required to maintain a steady state with equal nonzero amplitudes is the same for all frequency channels. Substituting Eq. (25) into Eq. (24), we arrive at the final form of the model:

$$\frac{d\eta_j}{dz} = 4\epsilon\eta_j\left[\frac{1}{3}\left(\eta^2 - \eta_j^2\right) + \frac{2}{T}\sum_{k=1}^{N}(1-\delta_{jk})(\eta-\eta_k)\right]. \tag{26}$$

The system (26) gives a complete description of the dynamics of soliton amplitudes in an N-channel transmission line. In population dynamics terminology it can be described as a Lotka-Volterra system for N competing species.

B. Amplitude dynamics in a two-channel system

As an example, let us consider in detail the dynamics of soliton amplitudes in a two-channel transmission system. In this case $g_1 = g_2 = 4\epsilon\eta(\eta/3 + 2/T)$, and Eq. (26) takes the form

$$\begin{aligned}\frac{d\eta_1}{dz} &= 4\epsilon\eta_1\left[\left(\eta^2 - \eta_1^2\right)/3 + 2(\eta-\eta_2)/T\right],\\ \frac{d\eta_2}{dz} &= 4\epsilon\eta_2\left[\left(\eta^2 - \eta_2^2\right)/3 + 2(\eta-\eta_1)/T\right].\end{aligned} \tag{27}$$

Equation (27) can have six equilibrium states with nonzero amplitude values in one or both channels. These equilibrium states are located at (η,η), $(0,0)$, $(C^{1/2}(\eta),0)$, $(0,C^{1/2}(\eta))$, $(C_2(\eta),C_3(\eta))$, and $(C_3(\eta),C_2(\eta))$, where $C(\eta) = \eta^2 + 6\eta/T$, $C_2(\eta) = 3/T + (C(\eta) - 27/T^2)^{1/2}$, and $C_3(\eta) = 3/T - (C(\eta) - 27/T^2)^{1/2}$. Table I summarizes the main properties of these equilibrium states. The first four equilibrium states exist for any $\eta > 0$, and the fifth and sixth equilibrium states exist provided that $3/T < \eta < 3(\sqrt{5}-1)/T$. Furthermore, linear stability analysis shows that (η,η) is a stable node (a sink) for $\eta > 3/T$, while for $0 < \eta < 3/T$ it is a saddle (unstable). In contrast, the equilibrium state at $(0,0)$ is an unstable node (a source) for any $\eta > 0$. The states $(C^{1/2}(\eta),0)$ and $(0,C^{1/2}(\eta))$ are saddles (unstable) when $\eta > 3(\sqrt{5}-1)/T$ and stable nodes (sinks) when $0 < \eta < 3(\sqrt{5}-1)/T$ [47]. Finally, the equilibrium points $(C_2(\eta),C_3(\eta))$ and $(C_3(\eta),C_2(\eta))$ are saddles (unstable) in the entire region of their existence. Based on this discussion we conclude that for a fixed value of T the system undergoes two bifurcations, one at $\eta = 3/T$ and another at $\eta = 3(\sqrt{5}-1)/T$. From a practical point of view, these observations mean that in order to maintain stable transmission with the same nonzero amplitude value η in both channels, the time slot width T has to be larger than $3/\eta$. Furthermore, for parameter values $\eta = 1$ and $T = 10$, which are typical for certain soliton-based WDM

transmission systems [48], $3/T < 3(\sqrt{5}-1)/T < \eta$. Thus, for these parameter values only the first four equilibrium states exist, and (1,1) is the only stable equilibrium state; i.e., stationary stable transmission with equal prescribed amplitude values is guaranteed by the above choice of the net linear gain coefficients.

The analytic predictions described in the previous paragraph were verified by numerical solution of Eq. (27). However, this does not tell us whether the assumptions that were used to derive the model are indeed satisfied. A more complete test for the validity of Eq. (27) should consist of numerical simulations with the full NLS model (1) or with an equivalent coupled-NLS model. Since the dynamics under consideration involves a large number of very frequent collisions, amplitude measurements are difficult to perform with the NLS model (1). Thus, we choose to work with the following equivalent coupled-NLS model:

$$\begin{aligned} &i\partial_z\psi_1 + \partial_t^2\psi_1 + 2|\psi_1|^2\psi_1 + 4|\psi_2|^2\psi_1 \\ &\quad = ig_1\psi_1/2 - i\epsilon|\psi_1|^2\psi_1 - 2i\epsilon|\psi_2|^2\psi_1, \\ &i\partial_z\psi_2 + \partial_t^2\psi_2 + 2|\psi_2|^2\psi_2 + 4|\psi_1|^2\psi_2 \\ &\quad = ig_2\psi_2/2 - i\epsilon|\psi_2|^2\psi_2 - 2i\epsilon|\psi_1|^2\psi_2. \end{aligned} \tag{28}$$

In Eqs. (28), ψ_1 and ψ_2 are the envelopes of the electric field in channels 1 and 2, respectively, and $g_1 = g_2 = 4\epsilon\eta(\eta/3 + 2/T)$. The terms $4|\psi_2|^2\psi_1$ and $4|\psi_1|^2\psi_2$ describe cross-phase modulation, $ig_1\psi_1/2$ and $ig_2\psi_2/2$ correspond to linear gain, $-i\epsilon|\psi_1|^2\psi_1$ and $-i\epsilon|\psi_2|^2\psi_2$ correspond to intrachannel effects due to cubic loss, while $-2i\epsilon|\psi_2|^2\psi_1$ and $-2i\epsilon|\psi_1|^2\psi_2$ describe interchannel effects due to cubic loss. The frequencies of the two channels in the numerical simulations are $\beta_1 = 0$ and $\beta_2 = 40$, the cubic-loss coefficient is $\epsilon = 0.01$, and the desired equilibrium value of the soliton amplitude is $\eta = 1$. The initial condition for the simulations is in the form of two periodic soliton sequences with amplitudes $\eta_1(0)$ and $\eta_2(0)$ and zero phase:

$$\begin{aligned} \psi_1(t,0) &= \sum_{j=-J}^{J} \frac{\eta_1(0)}{\cosh[\eta_1(0)(t-jT)]}, \\ \psi_2(t,0) &= \sum_{j=-J}^{J} \frac{\eta_2(0)\exp[i\beta_2(t-jT+T/2)]}{\cosh[\eta_2(0)(t-jT+T/2)]}, \end{aligned} \tag{29}$$

where $T = 10$ and $J = 3$ are used. Notice that in order to avoid dealing with incomplete collisions, soliton positions in channel 2 are initially shifted by $-T/2$ relative to soliton positions in channel 1.

Equations (28) are solved numerically using a split-step scheme similar to the one described in Sec. III. The use of periodic boundary conditions means that the numerical simulations mimic pulse dynamics in a closed waveguide loop. The size of the computational domain is $-35 \leqslant t \leqslant 35$, and the step sizes in t and z are $\Delta t = 0.015$ and $\Delta z = 0.001$, respectively. In order to test our predictions on transmission stability, the numerical simulations are carried out up to a final propagation distance $z_f = 180$. At this distance radiation emission effects are still small and all solitons retain their shape, as illustrated by Fig. 6, which shows the final pulse

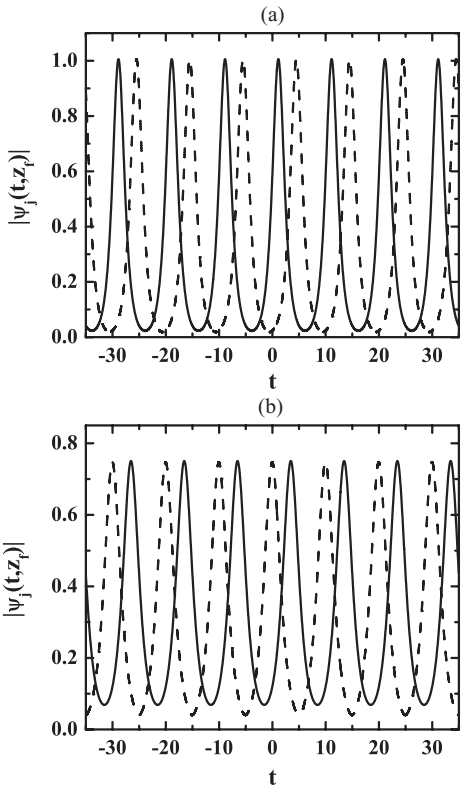

FIG. 6. The final pulse patterns in channels 1 and 2 $|\psi_1(t,z_f)|$ (solid line) and $|\psi_2(t,z_f)|$ (dashed line) as obtained by numerical integration of Eq. (28) with compensation of collision-induced loss (a) and without compensation of collision-induced loss (b). The parameter values are $\epsilon = 0.01$, $\beta_1 = 0$, $\beta_2 = 40$, $T = 10$, $\eta = 1$, and $z_f = 180$. The initial condition is $\eta_1(0) = 0.90$ and $\eta_2(0) = 0.95$.

patterns $|\psi_1(t,z_f)|$ and $|\psi_2(t,z_f)|$ for input amplitude values $\eta_1(0) = 0.90$ and $\eta_2(0) = 0.95$. The z dependence of the soliton amplitudes obtained by simulations with Eq. (28) is shown in Fig. 7 along with the result obtained by numerical solution of the Lotka-Volterra model [Eq. (27)]. Also shown is the result of numerical simulations with Eq. (28) without compensation of collision-induced loss, i.e., when the linear gain coefficients are $g_1 = g_2 = 4\epsilon\eta^2/3$. We consider three different initial conditions, $\eta_1(0) = \eta_2(0) = 1$ [Fig. 7(a)], $\eta_1(0) = 1.03$ and $\eta_2(0) = 0.97$ [Fig. 7(b)], and $\eta_1(0) = 0.90$ and $\eta_2(0) = 0.95$ [Fig. 7(c)]. In all three cases we observe good agreement between the result of the reduced model and the result obtained by numerical solution of Eq. (28) *with* compensation of collision-induced loss. In particular, for the initial condition $\eta_1(0) = \eta_2(0) = 1$, amplitude values obtained with Eq. (28) stay very close to 1, in accordance with the fact that (1,1) is an equilibrium state of Eq. (27). Similarly, for the other two initial conditions, $\eta_1(z)$ and $\eta_2(z)$ values tend toward 1 with increasing distance, in agreement with the linear stability of (1,1). Note that when collision-induced loss is not compensated, amplitude values decrease by about 25% at z_f, which illustrates that collision-induced loss is quite important already in two-channel transmission. It is also seen from Fig. 7 that even when collision-induced loss is not compensated, the amplitude values tend to an equilibrium state at (0.744,0.744). This result agrees with the result obtained by analyzing the

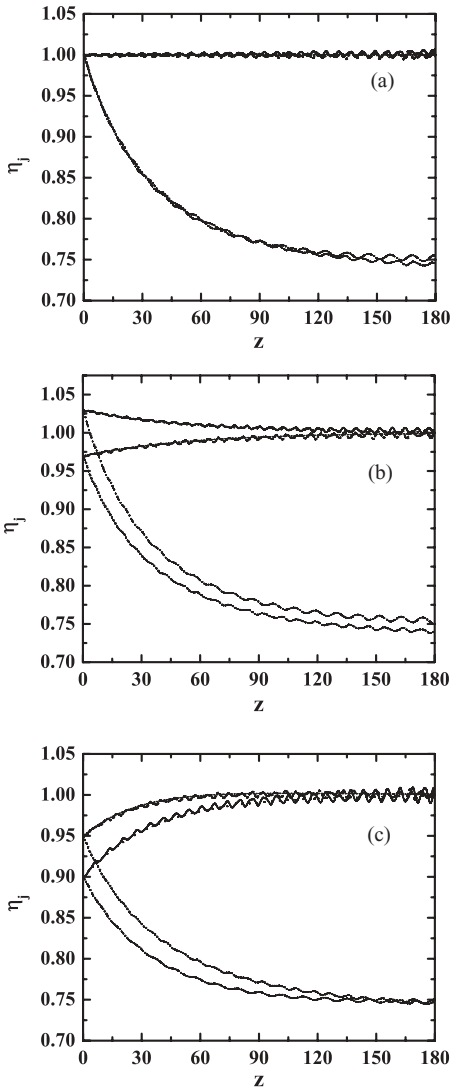

FIG. 7. The z dependence of soliton amplitudes in channels 1 and 2 for $\epsilon = 0.01$, $\beta_1 = 0$, $\beta_2 = 40$, $T = 10$, and $\eta = 1$. The initial amplitudes are $\eta_1(0) = \eta_2(0) = 1$ in (a), $\eta_1(0) = 1.03$ and $\eta_2(0) = 0.97$ in (b), and $\eta_1(0) = 0.90$ and $\eta_2(0) = 0.95$ in (c). The solid and dashed lines stand for $\eta_1(z)$ and $\eta_2(z)$ values obtained by numerical solution of the coupled-NLS model (28) with compensation of collision-induced loss. The dashed-dotted and short-dashed curves represent $\eta_1(z)$ and $\eta_2(z)$ values obtained by numerical solution of Eq. (28) without compensation of collision-induced loss. The dotted and short-dotted curves correspond to the result obtained with the reduced model (27).

corresponding Lotka-Volterra model with $g_1 = g_2 = 4\epsilon\eta^2/3$. Indeed, the analysis shows that the latter Lotka-Volterra model has a stable equilibrium state at $(C_4(\eta), C_4(\eta))$, where $C_4(\eta) = -3/T + (\eta^2 + 9/T^2)^{1/2}$. For the parameters used in the simulations $C_4(\eta) = 0.744$, in accordance with the curves presented in Fig. 7.

V. CONCLUSIONS

We investigated the dynamics of fast soliton collisions in a Kerr nonlinear waveguide with weak cubic loss ϵ. The cubic loss can result from two-photon absorption or from gain saturation. By employing a perturbation procedure with two small parameters ϵ and $1/|\beta|$, where β is the frequency difference, we obtained analytic expressions for the amplitude and frequency shifts induced by a single two-soliton collision. We showed that the collision-induced amplitude shift (cubic-loss cross talk) is proportional to $\epsilon/|\beta|$, while the cross-frequency shift scales like $\epsilon/(|\beta|\beta)$. These predictions were confirmed by numerical solution of the perturbed NLS equation with the cubic-loss term. Our analytic calculations and numerical simulations also showed that the total amplitude shift in two successive collisions is given by a sum of the amplitude shifts in each collision. Furthermore, for typical transmission systems, in which $|\beta| \gg 1$ and the amplitudes are of order 1, the amplitude shift in a fast three-soliton collision is given by a sum over the two-soliton interactions.

Based on these results we developed a reduced model for the evolution of soliton amplitudes in a broadband transmission line with N frequency channels. Assuming that the solitons in each frequency channel are well separated in time and neglecting radiation emission, we showed that amplitude dynamics is described by a Lotka-Volterra model for N competing species. For a two-channel system we showed that stable stationary transmission with equal nonzero amplitudes can be achieved by a proper choice of linear amplifier gain. Furthermore, transmission stability is fully characterized by the time slot width T and the equilibrium value of the soliton amplitude η. When $\eta > 3/T$ the transmission is stable, whereas when $\eta \leqslant 3/T$ it is unstable. The results of the reduced Lotka-Volterra model were confirmed by numerical simulations with a coupled-NLS model, which takes into account intrapulse and interpulse effects due to Kerr nonlinearity and cubic loss. We conclude by remarking that the closed waveguide-loop setup analyzed in Sec. IV might serve for stable energy equalization in broadband WDM transmission.

[1] G. P. Agrawal, *Nonlinear Fiber Optics* (Academic, San Diego, CA, 2001).
[2] A. H. Gnauck, R. W. Tkach, A. R. Chraplyvy, and T. Li, J. Lightwave Technol. **26**, 1032 (2008).
[3] L. F. Mollenauer and J. P. Gordon, *Solitons in Optical Fibers: Fundamentals and Applications* (Academic, San Diego, CA, 2006).
[4] Y. S. Kivshar and B. A. Malomed, Rev. Mod. Phys. **61**, 763 (1989).
[5] V. Mizrahi, K. W. DeLong, G. I. Stegeman, M. A. Saifi, and M. J. Andrejco, Opt. Lett. **14**, 1140 (1989).
[6] Y. Silberberg, Opt. Lett. **15**, 1005 (1990).
[7] A. B. Aceves and J. V. Moloney, Opt. Lett. **17**, 1488 (1992).
[8] G. S. He, J. D. Bhawalkar, C. F. Zhao, and P. N. Prasad, Appl. Phys. Lett. **67**, 2433 (1995).
[9] V. V. Afanasjev, J. S. Aitchison, and Y. S. Kivshar, Opt. Commun. **116**, 331 (1995).

[10] J. E. Ehrlich, X. L. Wu, I.-Y. S. Lee, Z.-Y. Hu, H. Röckel, S. R. Marder, and J. W. Perry, Opt. Lett. **22**, 1843 (1997).
[11] E. N. Tsoy, C. M. de Sterke, and F. Kh. Abdullaev, J. Opt. Soc. Am. B **18**, 1144 (2001).
[12] O. Katz, Y. Lahini, and Y. Silberberg, Opt. Lett. **33**, 2830 (2008).
[13] G. Tsigaridas, I. Polyzosa, V. Giannetasa, and P. Persephonisa, Chaos Solitons Fractals **35**, 151 (2008).
[14] A. Peleg, Y. Chung, T. Dohnal, and Q. M. Nguyen, Phys. Rev. E **80**, 026602 (2009).
[15] R. Soref, IEEE J. Sel. Top. Quantum Electron. **12**, 1678 (2006).
[16] M. A. Foster, A. C. Turner, J. E. Sharping, B. S. Schmidt, M. Lipson, and A. L. Gaeta, Nature (London) **441**, 960 (2006).
[17] Q. Lin, O. J. Painter, and G. P. Agrawal, Opt. Express **15**, 16604 (2007).
[18] R. Dekker, N. Usechak, M. Först, and A. Driessen, J. Phys. D **40**, R249 (2007).
[19] J. Zhang, Q. Lin, G. Piredda, R. W. Boyd, G. P. Agrawal, and P. M. Fauchet, Opt. Express **15**, 7682 (2007).
[20] M. A. Foster, A. C. Turner, M. Lipson, and A. L. Gaeta, Opt. Express **16**, 1300 (2008).
[21] W. Ding, C. Benton, A. V. Gorbach, W. J. Wadsworth, J. C. Knight, D. V. Skryabin, M. Gnan, M. Sorrel, and R. M. De La Rue, Opt. Express **16**, 3310 (2008).
[22] G. S. He, Q. Zheng, K.-T. Yong, F. Erogbogbo, M. T. Swihart, and P. N. Prasad, Nano Lett. **8**, 2688 (2008).
[23] O. Yoshitomo, O. Kuzucu, M. A. Foster, R. Salem, A. L. Gaeta, A. C. Turner-Foster, M. Lipson, A. Biberman, N. Ophir, and K. Bergman, in *Proceedings of the Optical Fiber Communication Conference, San Diego, CA, 2010* (Optical Society of America, 2010), paper JWA21.
[24] A. Peleg, M. Chertkov, and I. Gabitov, Phys. Rev. E **68**, 026605 (2003).
[25] A. Peleg, M. Chertkov, and I. Gabitov, J. Opt. Soc. Am. B **21**, 18 (2004).
[26] J. Soneson and A. Peleg, Physica D **195**, 123 (2004).
[27] Y. Chung and A. Peleg, Nonlinearity **18**, 1555 (2005).
[28] Y. Chung and A. Peleg, Phys. Rev. A **77**, 063835 (2008).
[29] J. S. Aitchison, A. M. Weiner, Y. Silberberg, M. K. Oliver, J. L. Jackel, D. E. Leaird, E. M. Vogel, and P. W. E. Smith, Opt. Lett. **15**, 471 (1990).
[30] H. H. Fan, Y. J. He, J. W. Dong, B. C. Chen, H. Z. Wang, Y. P. Tian, and M. F. Reid, Appl. Phys. Lett. **96**, 021109 (2010).
[31] V. E. Zakharov and A. B. Shabat, Zh. Eksp. Teor. Fiz. **61**, 118 (1971) [Sov. Phys. JETP **34**, 62 (1972)].
[32] M. N. Islam, ed., *Raman Amplifiers for Telecommunications 1: Physical Principles* (Springer, New York, 2004).
[33] C. Headley and G. P. Agrawal, eds., *Raman Amplification in Fiber Optical Communication Systems* (Elsevier, San Diego, CA, 2005).
[34] J. D. Ania-Castañón, T. J. Ellingham, R. Ibbotson, X. Chen, L. Zhang, and S. K. Turitsyn, Phys. Rev. Lett. **96**, 023902 (2006).
[35] R. Claps, D. Dimitropoulos, V. Raghunathan, Y. Han, and B. Jalali, Opt. Express **11**, 1731 (2003).
[36] Q. Xu, V. R. Almeida, and M. Lipson, Opt. Express **12**, 4437 (2004).
[37] R. Jones, H. Rong, A. Liu, A. Fang, M. Paniccia, D. Hak, and O. Cohen, Opt. Express **13**, 519 (2005).
[38] A. Hasegawa and Y. Kodama, *Solitons in Optical Communications* (Clarendon, Oxford, 1995).
[39] A. Peleg, Opt. Lett. **29**, 1980 (2004).
[40] A. Peleg, Phys. Lett. A **373**, 2734 (2009).
[41] Q. M. Nguyen and A. Peleg, J. Opt. Soc. Am. B **27**, 1985 (2010).
[42] D. J. Kaup, Phys. Rev. A **44**, 4582 (1991).
[43] M. Chertkov, Y. Chung, A. Dyachenko, I. Gabitov, I. Kolokolov, and V. Lebedev, Phys. Rev. E **67**, 036615 (2003).
[44] H. Yoshida, Phys. Lett. A **150**, 262 (1990).
[45] Q. M. Nguyen and A. Peleg, Opt. Commun. **283**, 3500 (2010).
[46] A. Peleg and Q. M. Nguyen, in *Proceedings of the Optical Fiber Communication Conference, San Diego, CA, 2010* (Optical Society of America, 2010), paper OMO1.
[47] Further analysis shows that (η,η) is unstable when $\eta = 3/T$ and that $(C^{1/2}(\eta),0)$ and $(0,C^{1/2}(\eta))$ are unstable when $\eta = 3(\sqrt{5}-1)/T$.
[48] L. F. Mollenauer and P. V. Mamyshev, IEEE J. Quantum Electron. **34**, 2089 (1998).